Pollution Control Policies and Natural Resource Dynamics: A Theoretical Analysis

Sergio Rinaldi*, Warren Sanderson‡ and Alessandra Gragnani†

* Research Centre for Environmental and Computer Sciences (C.I.R.I.T.A.), and † Department of Electronics and Information, Politecnico di Milano, Milano, Italy. ‡ International Institute for Applied Systems Analysis, A-2361 Laxenburg, Austria, on sabbatical leave from the Department of Economics, State University of New York at Stony Brook, Stony Brook, NY, U.S.A.

Policies for the management of natural resources and the resources themselves interact to form complex systems. In this paper, we present a highly simplified model that can be used to study the general features of those systems. The model has three state variables, the abundance of the resource, environmental pollution, and the capital devoted to pollution control. We analyse it graphically using the singular perturbation approach. Two modes of behavior are possible; stationary and cyclic. When the abundance of the resources varies cyclically, the length of the period of resource scarcity depends on population size, economic activity, pollution per unit of output, and policy constraints. We distinguish between two classes of policies, one in which decision-makers base their investments in pollution control capital on the abundance of the resource, and another in which those decisions depend on the amount of pollution. We show that policies based on the observation of pollution are safer than those based on resource abundance, because in the latter case, small changes in policy variables can lead much more easily to a collapse of the resource. Increases in population size, even when accompanied by an equiproportional increase in the pollution control budget can lead to a change from stationary to cyclic behavior, especially where policies are based on resource abundance.

© 1996 Academic Press Limited

1. Introduction

Natural resources are not always in a stationary regime. Indeed, a number of resources follow a cyclic regime, even when they are uncontaminated and unexploited. Recurrent pest outbreaks, fires in Mediterranean forests, and algal-blooms in water bodies are examples of natural cycles. However, exploitation and contamination enrich the spectrum of possible scenarios. Transitions from stationary to cyclic regimes, as well as

collapse of a resource due to a small increase of the exploitation effort or the concentration of a toxic substance, are well documented in fisheries, rangelands, aquatic, and forest ecosystems. But the dynamics of the resource become even more complex when exploitation and contamination vary in time. Often the dynamics of the biological and chemical components (resources and contaminants) of a given system influence the actions taken by institutions responsible for environmental protection and exploitation. For example, progressive acidification of lakes and forests has elicited a counteracting pollution control effort in a number of countries (International Institute for Applied Systems Analysis, 1993; United Nations Economic Commission on Europe, 1994).

Institutions and the economy interact with the environment, making the prediction of the dynamics of the resulting system a highly complex problem (Walters, 1986). These problems have been studied under many different circumstances and the models used share many common features. In this paper, we present a simple general model that incorporates some of the most important features and show how it can assist in policy formulation. In particular, we consider the case of a resource growing in a contaminated environment, but restrict our analysis by assuming that the economic activities that cause pollution flows are not directly related to the resource or its exploitation.

The model has only three state variables: the abundance of the resource, environmental pollution, and the capital devoted to pollution control. It is simple in four ways. First, the environmental system is composed of a unique resource influenced by one form of pollution only. Interactions between different resources and/or between different pollutants are ignored. Second, only two simple forms of pollution control policies are considered. Policy-makers are assumed to be ignorant of the details of the environmental system and are allowed to make decisions only on the basis of information on the resource abundance or the pollution level. Third, the socio-economic setting itself is highly simplified. Below, we consider how the levels of those variables influence the system, but the dynamics of changes in the number of people and pollution per person are ignored here. Fourth, the mathematics that we use to identify the dynamics of the system is relatively simple. Indeed, all the properties that we discuss are presented graphically, with the style used by Noy-Meir (1975) in his remarkable paper on grazing systems.

The model is general in the sense that it is designed to capture the major features shared by many environmental systems. Whenever possible, key relationships enter the model through characterizations of their properties rather than through specific functional forms. The result is a model that does not represent any specific system in full detail, but instead incorporates the core features of many.

The main disadvantage of a simple and general model is that it cannot, by its nature, produce new results for specific cases. Thus, virtually everything that we find has already been found in the study of one or a number of specific resources. The prime advantages of this approach are that we can see patterns that recur more clearly in the study of many resources and that we can discuss policy formulation in a general context.

There have been four main approaches to the study of natural resources and they can be described as entries in a two by two matrix. On one axis we have models that are analytic and those that are specified numerically. On the other axis, we have models that characterize policy decision rules with and without explicit optimization. (Notice that models that do not explicitly make use of optimization may, nevertheless, take into account the rationality of the agents involved.)

Numeric models with or without optimization (like linear programming models or simulation models) are used most often to answer specific questions. In the case of aquaculture, for example, Kishi *et al.* (1994) present a management simulation model applied to Mikame Bay in Japan, and Fisher *et al.* (1991) contains a model of a salmon fishery in California. Such models are suitable for their own purposes, but lack the generality that we seek here.

A good representative of the rich tradition of analytic models can be found in Clark (1990) where exploitation policies are systematically derived through optimal control theory. Those models provide us with certain insights. There are many cases, however, in which there may be conflicting demands on the environmental system, so that a policy that is optimal from one perspective may not be optimal from another. Second, and most important, environmental systems may not be completely understood; thus, it may be preferable to follow a simple, pragmatic, but robust policy (that assumes little knowledge of the system), rather than to follow a more complex policy derived through optimization, but based on an incorrect assessment. This is in line with the tradition of process control engineering, where despite the huge number of sophisticated criteria for designing optimal controllers, the most commonly used ones are still the so-called industrial controllers. These controllers are very simple and can be easily adapted to almost all situations, even if there is no clear understanding of the dynamics of the process.

In this paper, we specify *a priori* the structure of the control policy, thus avoiding the explicit use of any optimization criterion. This along with other simplifications produces an analytically tractable model that allows us to derive general results in a very transparent way. A purely geometric approach based on the *singular perturbation method* (Hoppensteadt, 1974; Muratori and Rinaldi, 1991) is used to show why and when the system will go to an equilibrium or to a limit cycle and to point out the circumstances in which there will be collapses and regenerations of the resource.

The results are: (1) there are two possible asymptotic modes of behavior: stationary or cyclic. The second involves periodic collapses and regenerations of the resource, which take place in a short period of time, and which are separated by relatively long periods of time during which the resource is either abundant or scarce.

(2) The length of the period during which the resource is scarce depends sensitively on the socio-economic setting, in particular population size, economic activity, pollution per unit of output, and policy constraints.

(3) Pollution control policies based on observations of environmental pollution are safer than those based on observation of resource abundance, because the former are less likely to lead to catastrophic collapses of the resource.

(4) Increasing population size, economic activity per capita, or other parameters can cause the system to change its behavior from stationary to cyclic. This is especially true in the case where policy is based on resource abundance.

But, in a sense, the main result is that all the above properties are derived from a simple and compact framework by using geometrical arguments only.

The model is presented in Section 2. We proceed with its analysis in three steps. In Section 3, we consider the dynamics of resource abundance and environmental pollution for a fixed amount of pollution control capital. The effects of using two classes of pollution control policies on the dynamics of the whole system are shown in Section 4. In Section 5, we describe the consequences of changes in population size, pollution per person, policy constraints, and stocking. The final section contains concluding remarks.

2. The model

The model has only three variables. The first, $R(t)$, is a measure of the abundance of the resource at time t. Important biological characteristics of the resource, like species diversity, age structure, and sex ratio, as well as spatial inhomogeneity, are not considered here. The second variable, $P(t)$, is a measure of the environmental pollution that influences the growth of the resource. The concentration of mobilized aluminum in the soil is a good example if the resource is tree biomass. Another example is the concentration of filamentous cyanobacteria (blue-green algae) if the resource is the amount of zooplankton supporting the fish stock in a shallow lake. The third variable, $C(t)$, is a measure of the capital devoted to pollution control at time t per unit of *potential pollution flow*. The potential pollution flow, indicated by w, is the flow of pollution that would be discharged into the environment in the absence of any pollution control effort. For example, in the case of a lake surrounded by a number of towns summing up to a population N, the potential pollution flow w would be N times the average amount of pollution produced per person in one day. Thus, $C(t)$ would be the value of the treatment plants active at time t divided by w. In other words, $C(t)$ would be (modulo a conversion factor) the pollution control capital per person used in treating wastewater.

Resource abundance, pollution, and pollution control capital interact and vary over time according to three simple differential equations:

$$\dot{R} = R(1 - R) - M(P)R + s \tag{1}$$

$$\dot{P} = wD(C) - aP - bPR \tag{2}$$

$$\dot{C} = -eC + fD(C)\pi(R, P) \tag{3}$$

where $\dot{R}$, $\dot{P}$, and $\dot{C}$ are the time derivatives of R, P, and C, respectively.

The first term on the right-hand side of Equation (1) is the basic logistic growth of the resource. Net growth per capita and carrying capacity have been put equal to one. This is always possible by suitably scaling time and the resource. The second term in that equation represents surplus mortality due to pollution. $M(P)$ is the *excess mortality rate* per capita and it is assumed to be negligible up to a threshold and then to increase quite sharply as pollution rises. In other words, M, M', and M'' are non-negative. This is shown in Figure 1(a), where the threshold value of P has been assumed equal to unity (this can always be done by suitable scaling). We make no further assumptions about the mortality rate function. We will show below that the sharpness of that function will be an important determinant of the system's dynamic behavior. The last term in Equation (1), s, represents an exogenous increase in the resource due to immigration or to stocking.

Equation (2) is a mass-balance equation. The first term on the right-hand side is the inflow of pollution. It is the product of w, the amount of pollution produced in a time unit, and $D(C)$, the fraction of that flow that enters the environment. We call $D(C)$ the *pass-through function*, being the fraction of the pollution produced that is passed through to the environment. The pollution inflow, which would be equal to w in the absence of any pollution control capital, is reduced to $wD(C)$ if the pollution
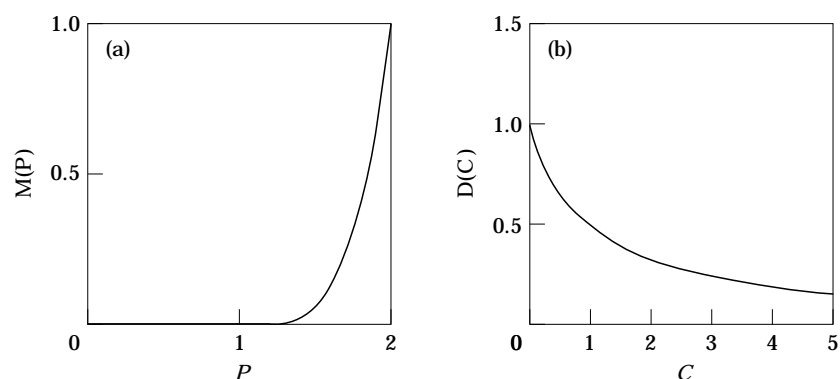
Figure 1. The shape of the two functions appearing in Equations (1) and (2): (a) the excess mortality function $M(P)$; (b) the pass-through function $D(C)$.

control capital is C. The function $D(C)$ is typically as in Figure 1(b), i.e. $D(0) = 1$, $D(\infty) = 0$, $D' < 0$. Moreover, we assume that there are *diminishing returns* to pollution control effort, and therefore that $D'' > 0$ (see, for example, Rinaldi *et al.* (1979) for the case of wastewater treatment). The second term in Equation (2) represents natural losses and self-purification processes. The equation assumes that such processes are linearly related to pollution. The third term is the amount of the pollutant taken up by the resource itself. Therefore, it is proportional both to the abundance of resource and the amount of pollution (see, for example, Gatto and Rinaldi (1987) for the case of forest ecosystems).

The third equation determines the net investment in new pollution control capital per unit of potential pollution flow. The first term on the right-hand side of the equation is the depreciation of pollution control capital, which is assumed to take place at a fixed rate, e. In our model, the policy-maker has the choice of how much to invest in pollution control. That choice, the amount of gross investment, is reflected in the second term and is itself the product of three terms: the constant parameter f, representing the maximum possible investment in pollution control (determined by the level of economic activity, the political situation, and other forces), the pass-through function $D(C)$ already discussed in Section 2, and the perception $\pi(R, P)$ of the seriousness of the problem. For all feasible values of R and P the function $\pi(R, P)$, from now on called *perception function*, lies between zero and unity and decreases (increases) with the amount of resource (pollution).

Equation (3) says that at any instant the policy-maker spends more on pollution control capital when the available budget (f) is higher, when the amount of pollution reaching the environment ($wD(C)$) increases, when the abundance of the resource decreases ($\partial \pi/\partial R < 0$), and when the stock of pollution increases ($\partial \pi/\partial P > 0$). The policy-maker knows the available budget, the shape of the pass-through function, and the amount of pollution control capital that is on-line. In addition, the policy-maker monitors the abundance of the resource and the amount of pollution and uses experience, intuition, and whatever else is helpful to decide on an expenditure level. Nevertheless, Equation (3) assumes that the decision-maker does not know the parameters of the biological and biochemical components of the system (Equations (1) and (2)). This rules out all forms of decision-making, such as optimal control, where knowledge of the parameters of the environmental system is required. In other words, Equation (3)
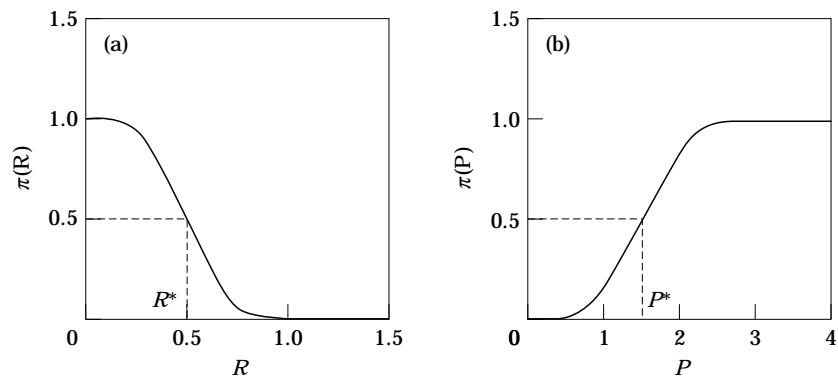
Figure 2. The two types of perception functions considered in the paper: (a) R-policy; (b) P-policy.

assumes that decision-making is made with incomplete knowledge of the underlying details of the relationships between resources and pollutants. We believe that this is commonly the case.

In our model, we make one further simplification. We consider only two classes of "extreme" perception functions, one in which π depends only on the abundance of the resource, R, and the other in which it depends only on the amount of pollution in the environment, P. We call the class of policies derived from using perception functions that depend only on the abundance of the resource *R-policies*, and the others *P-policies*. We make this distinction between R-policies and P-policies for two reasons. First, it is relevant for the policy formulation process. Decision-makers need to know the pros and cons of waiting until there is observed degradation of the resource to act as opposed to acting upon the evidence of pollution, possibly even before degradation appears. Second, as we show below, the two classes of policies can result in quite different consequences.

The two perception functions $\pi(R)$ and $\pi(P)$ are assumed to be shaped as in Figure 2. The first one, $\pi(R)$, is equal to unity when resource abundance is very low, and then decreases, approaching zero when the resource is at its carrying capacity or close to it. Obviously, this makes sense if a rough estimate of the carrying capacity is available to decision-makers, a condition which is often satisfied in practice. The abundance of the resource at which the perception is $1/2$ is indicated by R^*. If the π function is quite sharp around this point, then the investment policy is essentially a bang-bang policy, i.e. no investment if $R > R^*$ and maximum investment if $R < R^*$. We use R^* as an attribute of the R-policy in our discussion below.

Similarly, the perception function $\pi(P)$ increases with pollution and is equal to zero when P is low and equal to one when P is high. Of course, "low" and "high" here indicates low and high with respect to the values of pollution for which some impact on the resource is detectable. Thus, perception functions of this kind make sense only when the influence of pollution is at least roughly known.

3. Environmental dynamics with constant pollution control capital

In this section, we consider the dynamics of the model in the simple case where the pollution control capital is constant. Before we begin, it is important to stress that the
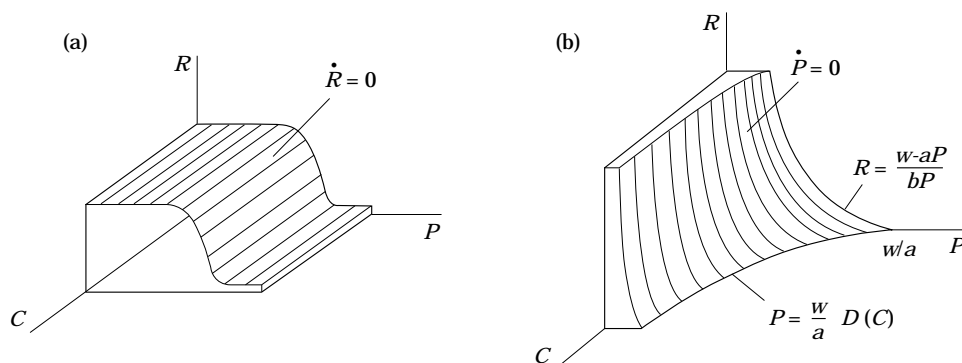
Figure 3. The manifolds $\dot{R}=0$ (a) and $\dot{P}=0$ (b) of model (1, 2). The figures have been obtained for the excess mortality function $M(P)$ and the pass-through function $D(C)$ shown in Figure 1 and for $a=0\cdot2$, $b=0\cdot2$, $s=0\cdot01$, $w=1$.

model in Equations (1) and (2) is a very crude representation of the growth of a natural resource. The list of phenomena which are not taken into account by these equations would be desperately long. Indeed, the number of equations used to simulate the growth and decay of resources like forests, crop production systems, and fisheries usually falls in the range of 10 to 100. On the other hand, even the addition of a single extra equation would give rise to an analytically untractable problem. The low dimension of the model is therefore dictated by the ultimate aim of the study, namely the formal derivation of general principles on resource/pollution/policy interactions.

Since the model in Equations (1) and (2) cannot have limit cycles (see the Appendix for a short proof based on Dulac's criterion), only its equilibria must be determined to qualify its asymptotic behavior. For this, let us consider the two manifolds $\dot{R}=0$ and $\dot{P}=0$ in the space (C, R, P). The manifold, $\dot{R}=0$, is described by the equation $R(1-R)+M(P)R+s=0$ and is therefore shaped like the surface in Figure 3(a). In particular, for high values of P, it approaches the (C, P) plane.

The second manifold, $\dot{P}=0$, is described by the equation $wD(C)-aP-bPR=0$ and is shaped like the surface in Figure 3(b). It approaches the (C, R) plane for low values of P and intersects the (C, P) plane along the curve $P=(w/a)D(C)$ and the (R, P) plane along the curve $R=(w-aP)/bP$. These two curves intersect one another on the P-axis at the point with coordinate w/a.

The *equilibrium manifold* of system (1, 2), i.e. the curve of the equilibria of system (1, 2) for all possible constant values of C, is the intersection of the above two manifolds. Depending upon the non-linearities involved in the model two distinct cases are possible. Figure 4(a) refers to the case in which the mortality function $M(P)$ and the pass-through function $D(C)$ are those in Figure 1. Figure 4(b), on the contrary, corresponds to weaker non-linearities. It has been obtained with the same pass-through function but with a mortality function raising up linearly after the threshold value $P=1$ and with the same average mortality over the range of interest $1 \leqslant P \leqslant 2$. In case (a), for high values of pollution control capital, C, there exists only one equilibrium with a high level of resource R and a low value of pollution P. Also, for low values of C there exists only one equilibrium but with scarce resource and high pollution. Finally, for intermediate values of C there exist three equilibria: two of them are stable and the third is a saddle (the proof of this fact follows directly from the analysis of the Jacobian
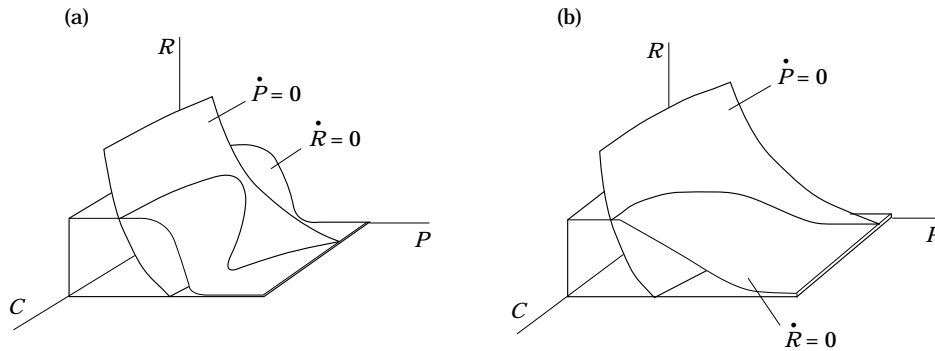
Figure 4. The equilibrium manifold of system (1, 2) is the line obtained by intersecting the manifolds $\dot{R}=0$ and $\dot{P}=0$. Case (a) corresponds to the functions and parameters specified in the caption of Figure 3. Case (b) corresponds to an excess mortality function which is linearly increasing for $P>1$ and has the same average as the function shown in Figure 1(a) in the range $1 \leqslant P \leqslant 2$.
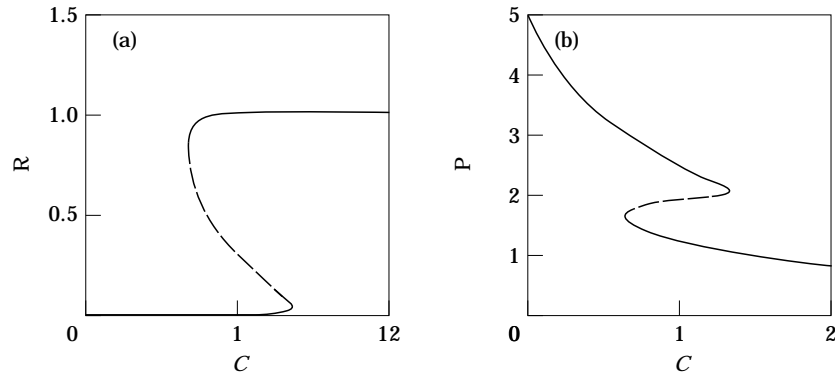

Figure 5. The projection of the equilibrium manifold of Figure 4(a) on the (C, R) plane (a) and on the (C, P) plane (b). These graphs illustrate hystereses. The upper and lower branches (continuous lines) correspond to stable equilibria, while the dashed part corresponds to unstable equilibria.

of system (1, 2)). Trajectories tend toward one or the other of the stable equilibria depending upon their initial conditions. On the contrary, in case (b), multiple equilibria are not present: for each value of C the system has only one equilibrium which is globally stable.

The projections of the equilibrium manifold of Figure 4(a) in the (C, R) plane and in the (C, P) plane are shown in Figure 5. This graph, known as *hysteresis*, shows that a variation of the pollution control capital C can give rise to "catastrophic" transitions. For example, let us make reference to Figure 5(a), and assume that C is high and that the system is at equilibrium. Thus, the resource is abundant and the pollution is relatively low. Decrease C very slowly over time and resource and pollution will also vary very slowly along the upper branch of the hysteresis, thus approaching the point where the hysteresis is folded. If C is decreased further, that point will be passed and the system will undergo a transition from the upper to the lower branch of the hysteresis. In other words, the resource will collapse. Once the system is on the lower branch of the hysteresis it remains on that branch even if the pollution control capital is slightly
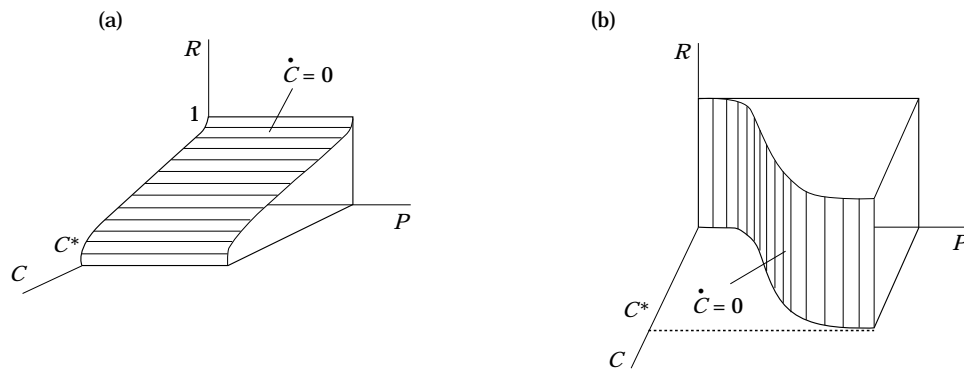
Figure 6. The equilibrium manifold $\dot{C}=0$ of the slow subsystem (Equation (3)) for the pass-through function of Figure 1(b) and $f/e=5$ and for the two perception functions shown in Figure 2: (a) R-policy; (b) P-policy.

increased. The resource can be regenerated through a transition from the lower to the upper branch of the hysteresis only if C is increased so much that the right fold is overcome.

4. Environmental dynamics with variable pollution control capital

The dynamic behavior of system (1–3) will be analysed assuming that C varies much more slowly than R and P. This assumption is justified in a great number of cases, because of the limited funds that are available for investment at any time and because there are often important social and organizational constraints on how quickly new capital can be brought into use. Technically speaking, this is the case if the two positive parameters e and f in Equation (3) are small. A relatively small e means that the pollution control capital does not depreciate rapidly. A relatively small f means that the budget for pollution control capital is small so that the pollution control capital can be increased only marginally in the short-term.

If C varies much more slowly than R and P, then the singular perturbation method (Hoppensteadt, 1974) can be applied. This approach has very often been advocated and used in ecology (see, for example, May, 1977; Ludwig *et al.*, 1978; Berryman and Stenseth, 1984; Holling, 1986; Rinaldi and Muratori, 1992*a*,*b*) to point out the consequences of the interactions between very small (or fast) and very big (or slow) components of complex ecosystems. Such a method says that the time evolution of the system is well approximated by the concatenation of alternate fast and slow transients. In the present case, the fast transients are time evolutions of R and P obeying Equations (1) and (2) with constant C. Such fast transients could therefore be visualized in the three-dimensional space (C, R, P) as trajectories developing in a plane where C is constant and tending toward a stable equilibrium point of the fast system, namely toward a point of the curve $\dot{R}=\dot{P}=0$ shown in Figure 4. Once the state of the system is on this curve it will move along it very slowly, obeying Equation (3). Of course, the direction in which the system moves is dictated by the sign of $\dot{C}$. For this reason it is very useful to visualize the manifold $\dot{C}=0$ which divides the state space into two regions: one in which the slow motion is characterized by increasing values of C and the other where C decreases. Such manifold is shown in Figure 6 for the two perception
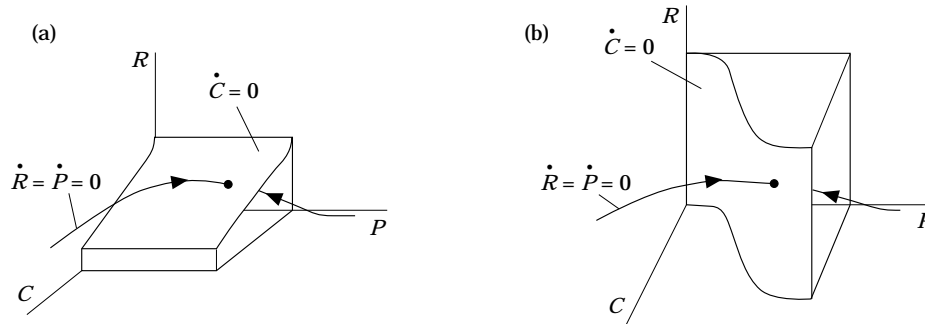
Figure 7. The equilibrium manifold $\dot{R}=\dot{P}=0$ of the fast subsystem (1, 2) and the equilibrium manifold $\dot{C}=0$ of the slow subsystem (3). The state of the system moves very slowly along the manifold $\dot{R}=\dot{P}=0$ and tends toward an equilibrium. The figure corresponds to the case of no hysteresis shown in Figure 4(b): (a) R-policy (see Figure 6(a)); (b) P-policy (see Figure 6(b)).

functions of Figure 2. Notice that this manifold does not depend upon e and f separately, but only upon their ratio f/e.

   If the fast system has no multiple equilibria (see Figure 4(b)), the slow transient ends at an equilibrium point, as explicitly shown in Figure 7. On the contrary, when the fast system has multiple equilibria (see Figure 4(a)) different scenarios are possible. Some of them involve the collapse and/or the regeneration of the resource or even a *slow–fast limit cycle*, i.e. an infinite sequence of concatenated slow and fast transients, where the fast ones are alternatively associated with the collapse and the regeneration of the resource. We present first the results for R-policies followed by those for P-policies.

4.1. R-POLICIES

When the perception function depends only upon the abundance of the resource, the manifold $\dot{C}=0$ is sloping downward in the space (C, R). In other words, the function $R(C)$ defined by Equation (3) with $\dot{C}=0$ is decreasing. This is obviously true in general, since this manifold gives the pollution control capital C that one should expect at equilibrium if the resource R could be kept constant. A formal proof of this property can be given by letting $R=R(C)$ in Equation (3) with $\dot{C}=0$ and then taking the derivative with respect to C, i.e.:

$$-e+f\frac{dD}{dC}\pi(R)+fD(C)\frac{d\pi}{dR}\frac{dR}{dC}=0$$

which implies $dR/dC<0$ since $dD/dC<0$ and $d\pi/dR<0$. Figure 8 shows three typical scenarios corresponding to three different values of the ratio f/e. In case (a) the manifold $\dot{C}=0$ intersects the equilibrium manifold $\dot{R}=\dot{P}=0$ of the fast system at point E_1 on the upper branch of the hysteresis. Thus, all trajectories (two of which, starting from points 1 and 2, are indicated in the figure) tend to this equilibrium. Notice, however, that some of these trajectories, like that starting from point 2, involve the collapse of the resource (vertical fast trajectory going from point 2 to the C axis) and the regeneration of the resource (vertical fast trajectory going from point C to point D).
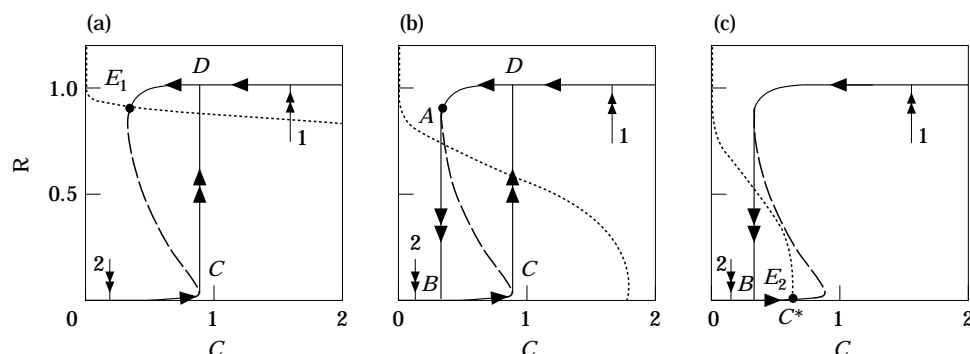
Figure 8. Slow (single arrow) and fast (double arrow) trajectories of system (1–3) with small values of e and f in the case of R-policy. Case (a): the manifold $\dot{C}=0$ with $f/e=50$ (dotted line) intersects the upper branch of the hysteresis at point E_1 and all trajectories tend toward this equilibrium point. Case (b): the manifold $\dot{C}=0$ with $f/e=5$ separates the two stable branches of the hysteresis and all trajectories tend toward a slow–fast limit cycle $ABCD$. Case (c): the manifold $\dot{C}=0$ with $f/e=1$ intersects the lower branch of the hysteresis at point E_2 and all trajectories tend toward this equilibrium point. The values of the parameters are: $a=0\cdot2$, $b=0\cdot2$, $s=0\cdot01$, $w=0\cdot8$.

In case (b) the manifold $\dot{C}=0$ separates the two branches of the hysteresis, so that a slow–fast limit cycle $ABCD$ exists. Moreover, all trajectories (like those starting from points 1 and 2) tend toward this cycle, which is therefore globally stable. (The interested reader can refer to Muratori and Rinaldi (1991) for details on the *separation principle*.) In such a case the resource is in general either quite abundant or almost absent and the periods of abundance and scarcity are very long, in comparison with the periods of collapse (vertical fast trajectory AB) and regeneration (vertical fast trajectory CD). Finally, in the third case the manifold $\dot{C}=0$ intersects only the lower branch of the hysteresis, so that all trajectories tend toward a stable equilibrium E_2 characterized by extreme scarcity of the resource.

The situation shown in Figure 8(b), involving slow–fast limit cycles, seems to be the most likely to occur. Indeed, Figure 8 indicates that for a wide range of the values of ratio f/e the situation is as in case (b).

Of course, for suitable values of the parameters, the manifold $\dot{C}=0$ can intersect the equilibrium manifold of the fast system at three points. In such a case there would be two alternative stable equilibria, one (E_1) with the resource abundant and the other (E_2) with the resource scarce. We do not analyse this situation because it is rather complex and requires, in any case, quite extreme perception functions.

4.2. *P*-POLICIES

When the perception function depends upon pollution as in Figure 2(b) the main scenarios are similar to those shown in Figure 9. Two of them (Figures 9(a) and 9(c)) are characterized by a unique stable equilibrium point. This equilibrium can have either a low pollution level (and consequently an abundant resource) as point E_1 (Figure 9(a)) or a high pollution level (and hence a very scarce resource) as point E_2 (Figure 9(c)). On the contrary, the intermediate scenario is characterized by the existence of two alternative stable equilibria E_1 and E_2. Thus, the collapse of the resource cannot be endogenously generated: it can only be the consequence of a severe pollution accident or of an unexpected failure of the treatment facilities, bringing the state of the system
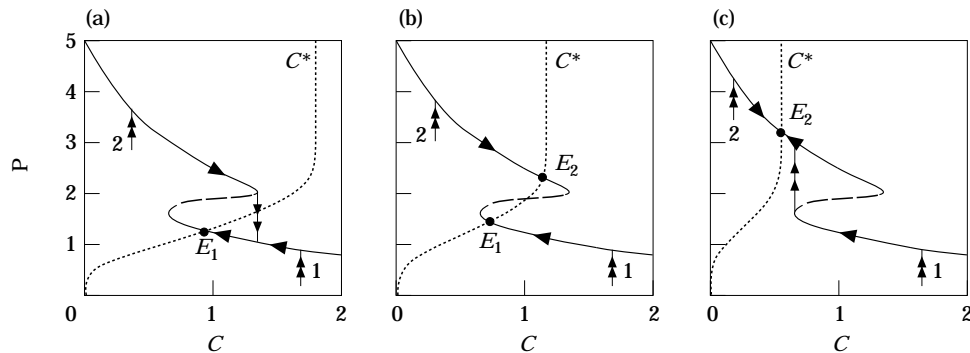
Figure 9. Slow (single arrow) and fast (double arrow) trajectories of system (1–3) with small values of e and f in the case of P-policy (see Figure 2(b)). Case (a): the manifold $\dot{C}=0$ with $f/e=5$ (dotted line) intersects the lower branch of the hysteresis at point E_1 and all trajectories tend toward this equilibrium point. Case (b): the manifold $\dot{C}=0$ with $f/e=2\cdot5$ intersects both stable branches of the hysteresis at points E_1 and E_2 and some trajectories tend toward E_1 while others tend toward E_2. Case (c): the manifold $\dot{C}=0$ with $f/e=1$ intersects the upper branch of the hysteresis and all trajectories tend toward this equilibrium point. The values of the parameters are $a=0\cdot2$, $b=0\cdot2$, $s=0\cdot01$, $w=1$.

from the equilibrium E_1 into the basin of attraction of the alternative equilibrium E_2.

Mathematically speaking, the case in which the manifold $\dot{C}=0$ separates the two stable branches of the hysteresis (and therefore in which slow–fast limit cycles exist) is also possible. Nevertheless, this situation requires the use of a sharp perception function, a low depreciation (e), in comparison with maximum investment rate (f), and a level P^* (see Figure 2(b)) very close to the pollution level at which the resource cannot grow (because the upper branch of the hysteresis shown in Figure 9 corresponds to virtual extinction of the resource). For all these reasons it is very unlikely that the resource would collapse if P-policies are used. Nevertheless, P-policies can be very unpopular because they might require a consistent economic effort before any sign of deterioration of the resource is detectable. On the contrary, R-policies are more popular but the previous analysis has shown that a poor understanding of the behavior of the system, giving rise to a poor design of the pollution control actions, can be quite dangerous if used.

5. Influence of economy and of pollution control policy

In this section, we consider the influence of the economy and of the pollution control policy on the dynamic behavior of system (1–3).

Assuming that the system is at equilibrium with an abundant resource and low pollution and that the decision-maker uses R-policies, an increase in the potential pollution flow w, such as might arise from an increase in population size or an increase in economic activity per person, could trigger a transition to a cyclic regime. In fact, the graph $\dot{C}=0$ in the (C, R) plane (see Figure 8(a)) is not influenced by w, because w does not appear in Equation (3). On the other hand, given an equilibrium (R, P) of system (1, 2) where C is considered as a parameter, if w increases, then, from Equation (2) with $\dot{P}=0$, it follows that $wD(C)$ must remain constant, i.e. C (see Figure 1(b)) must increase. This means that the hysteresis, shown in Figure 8(a), shifts to the right. Thus, if w increases sufficiently, the graph $\dot{C}=0$ will separate the two stable branches of the hysteresis and a slow–fast limit cycle will appear. Consequently, increasing w
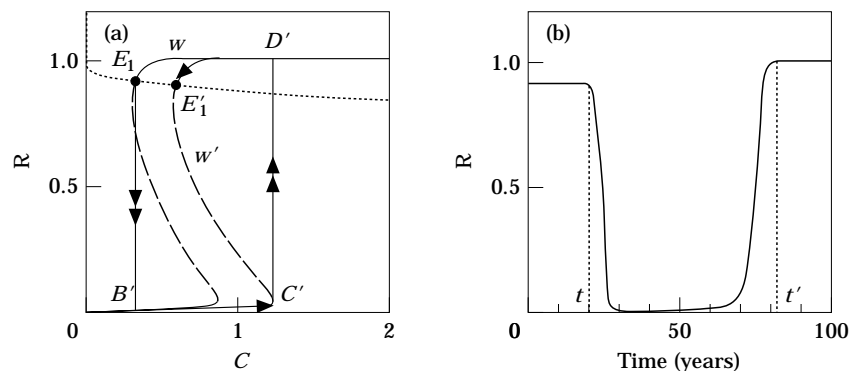
Figure 10. Collapse and regeneration of the resource due to an increase of the potential pollution flow w. The two hystereses shown in (a) correspond to two different values of the potential pollution flow, $w = 0.8$ and $w' = 0.96$, while the manifold $\dot{C} = 0$ (dotted line) corresponds to $f/e = 5$. If e and f are small and the potential pollution flow is increased from w to w', the system tends toward the new equilibrium E'_1 through a sequence of fast and slow transients $E_1 B' C' D' E'_1$. The time pattern of the resource for $e = 0.01$ and $f = 0.05$ is shown in (b) where t is the time at which the potential pollution flow is increased and t' is the time at which the resource is regenerated (see point D' in (a)).

from a value corresponding to an equilibrium for system (1–3) to a value corresponding to a slow–fast limit cycle, implies first the collapse of the resource, then a long period of scarce resource and, finally, the regeneration initiating the slow–fast cycle.

Sudden collapses of the resource may also occur even if the increase in w does not produce slow–fast cycles. For example, Figure 10 shows the case in which a 20% increase of w gives rise to the collapse of the resource followed by a long period of scarcity before regeneration finally takes place.

The influence of w on the slow–fast limit cycle is also quite easy to detect. As mentioned above, when w is increased, the hysteresis shifts to the right and its lower branch becomes closer and closer to the manifold $\dot{C} = 0$. This means that $\dot{C}$ becomes smaller and smaller on this branch and this implies that the period of time separating collapses and regenerations increases with w. Figure 11 confirms this analysis showing the limit cycles corresponding to three different values of w and to small values of e and f.

We now consider the effects of two parameters of an R-policy, namely R^* (the amount of resource at which the perception $\pi(R)$ is 1/2) and f (the maximum investment rate). The analogous discussion for P-policy is left to the reader.

The influence of R^* on system (1–3) can be easily seen in the case of an extremely sharp perception function $\pi(R)$. In fact, in such a case, if R^* decreases, the manifold $\dot{C} = 0$ in Figure 8(a) will shift downward and will therefore eventually separate the two stable branches of the hysteresis, thus giving rise to a cyclic regime. The conclusion is that low R^* values are dangerous.

The influence of f on system (1–3) can also be predicted by looking at its influence on the manifold $\dot{C} = 0$. For fixed R, an increase of f implies an increase of C (see Equation (3) with $\dot{C} = 0$), i.e. the manifold $\dot{C} = 0$ shifts to the right. Therefore, lowering f can cause a transition from a stationary to a cyclic regime. In other words, too low a value of the budget can also be dangerous.

If the number of people increases, we would expect that both w and f would increase (all other things being equal, a larger population would pollute more, but would also
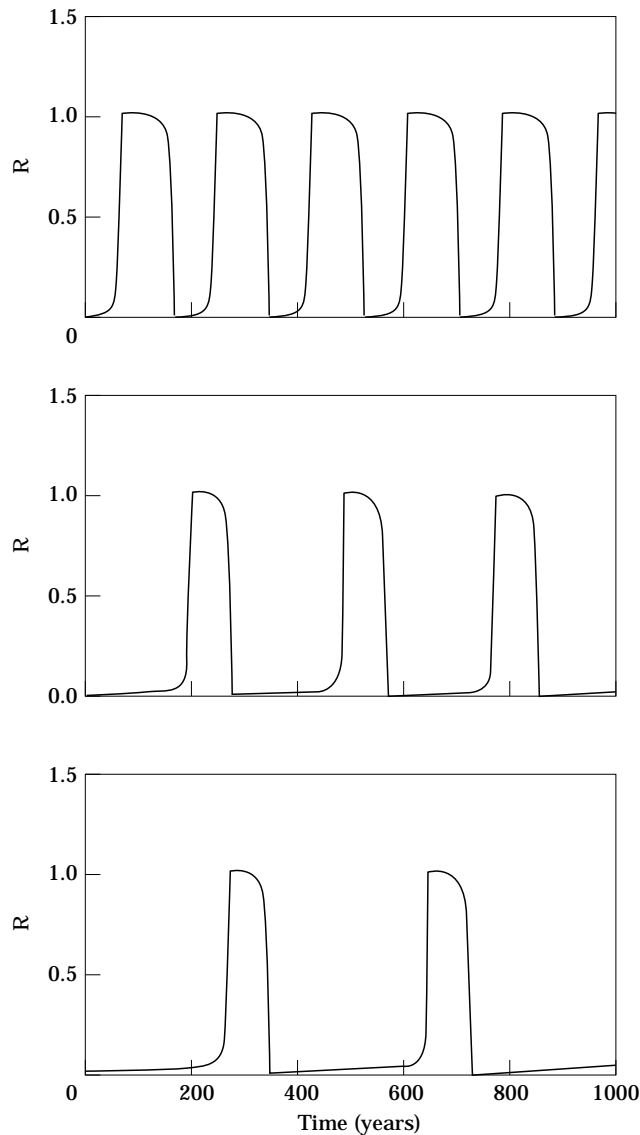
Figure 11. In a cyclical regime, the period during which the resource is scarce increases with the potential pollution flow ($w=1$; $1\cdot16$; $1\cdot18$ from top to bottom). The figure has been produced using the functions of Figure 1, the R-policy of Figure 2(a) and the parameter values $a=0\cdot2$, $b=0\cdot2$, $s=0\cdot01$, $e=0\cdot01$, $f=0\cdot05$.

have the resources to invest more in pollution control). Figure 12(a) (obtained through simulation) shows the influence of w and f on system (1–3). To the left of the curve, the system is stationary; to the right, it is cyclic. Imagine a system characterized by $w=0\cdot5$ and $f=0\cdot1$. In this case, the system will go to an equilibrium. Now if the number of people doubles, so that $w=1\cdot0$ and $f=0\cdot2$, the system will exhibit cycles with collapses and regenerations of the resource. Thus, an increase of population size can cause an abrupt transition from stationary to cyclic behavior.

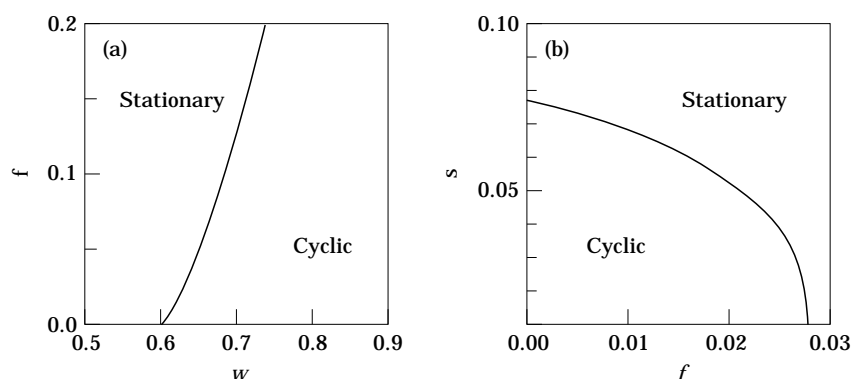In order to mitigate the negative effects induced by a reduction of f, one can increase

Figure 12. The regions of stationary and cyclic regimes in parameter space. The curves separating the two regions have been obtained through simulation, using the functions of Figure 1, the R-policy of Figure 2(a) and the parameter values $a=0.2$, $b=0.2$, $e=0.01$. Moreover, in (a) $s=0.01$, while in (b) $w=0.63$.

s by stocking, if this is feasible. In fact an increase of s (see Equations (1) and (2) with $\dot{R}=0$ and $\dot{P}=0$) shifts the hysteresis of Figure 8(a) to the left while a reduction of f shifts it to the right. Figure 12(b) confirms this possibility, by representing the curve in the plane (f, s) (obtained through simulation) that separates the stationary and cyclic regimes.

6. Conclusions

In this paper, we introduce a simple third-order model of the interactions between resource abundance (R), pollution (P), and pollution control capital (C), and show that its behavior can be analysed graphically using the singular perturbation approach. The model produces two types of behavior, stationary and cyclic. In the latter case, the resource goes through periods of growth and collapse punctuated by long periods of abundance or scarcity. We distinguish between two classes of environmental policies, one in which decision-makers base investments in pollution control on the abundance of the resource, R-policies, and another in which they base their decisions on the amount of pollution they observe, P-policies. We show that it is safer for decision-makers to focus on pollution rather than on the abundance of the resource because under R-policies small changes in one element of the policy mix can cause a discontinuous change from a high resource equilibrium to a cycle that begins with an almost total collapse of the resource. Increases in population, economic activity, or technological changes can also cause such a discontinuous change, even when they are accompanied by a proportional increase in the amount of funds available for pollution control. On the contrary, when P-policies are used, the system is much more difficult to crash.

Our analysis can be expanded in a number of directions. For example, if the dynamics of the resource depends upon the pollution flow ($wD(C)$ in Equation (2)), as in the case of trees with leaves damaged by acidic precipitation, the same model can be used, provided the dependence of the excess mortality of the resource upon the pollution flow is specified. This corresponds to an assumption that M in Equation (1) is a suitable function of $wD(C)$. Then, the same geometric approach used in this paper can be followed, assuming again that the pollution control capital varies much more slowly than R and P. Another interesting extension would be to consider more

sophisticated decision support systems. For example, one could assume that information on both R and P is available to the decision-maker who can then use (R, P)-policies (instead of R-policies or P-policies) to decide how much to invest in pollution control. Again, our geometric approach could be used to analyse the consequences of any specified (R, P)-policy. But the same approach can also be used to solve an interesting inverse problem, namely the determination of an (R, P)-policy which is at the same time safe (as the P-policies) and popular (as the R-policies). Finally, one could also try to extend the present study by modeling in a more accurate way one (or more) of the compartments of the system. For example, one could study the case in which the resource is the top component of a three-level food chain, thus using three differential equations to describe the dynamics of R. Leaving the rest unchanged, the resulting system would be of order 5. The singular perturbation approach could still be applied to it, under the assumption that P and the three components of the food chain vary more quickly than C. Nevertheless, the analysis would certainly be less transparent, because the high dimensionality of the model would destroy the possibility of showing the results by means of simple graphs, as done in this paper.

References

Berryman, A. A. and Stenseth, N. C. (1984). Behavioral catastrophies in biological systems. *Behavioral Science* **29**, 127–137.

Clark, C. W. (1990). *Mathematical Bioeconomics: The Optimal Management of Renewable Resources.* New York: John Wiley & Sons.

Fisher, A. C., Hanemann, W. M. and Keeler, A. G. (1991). Integrating fishery and water use management: a biological model of a California salmon fishery. *Journal of Environmental Economics and Management* **20**, 234–261.

Gatto, M. and Rinaldi, S. (1987). Some models of catastrophic behavior in exploited forests. *Vegetatio* **69**, 213–222.

Holling, C. S. (1986). The resilience of terrestrial ecosystems: local surprise and global change. In *Sustainable Development of the Biosphere* (W. C. Clark and R. E. Munn, eds), pp. 292–317. Cambridge, U.K.: Cambridge University Press.

Hoppensteadt, F. (1974). Asymptotic stability in singular perturbation problems. *Journal of Differential Equations* **15**, 510–521.

International Institute for Applied Systems Analysis. (1993). Acidification: modeling transboundary air pollution. *Options.* Winter. Laxenburg, Austria.

Kishi, M., Uchiyama, J. M. and Iwata, Y. (1994). Numerical simulation model for quantitative management of aquaculture. *Ecological Modelling* **72**, 21–40.

Ludwig, D., Jones, D. D. and Holling, C. S. (1978). Qualitative analysis of insect outbreak systems: the spruce budworm and forest. *Journal of Animal Ecology* **47**, 315–332.

May, R. M. (1977). Thresholds and breakpoints in ecosystems with a multiplicity of stable states. *Nature* **269**, 471–477.

Muratori, S. and Rinaldi, S. (1991). A separation condition for the existence of limit-cycles in slow–fast systems. *Applied Mathematical Modelling* **15**, 312–318.

Noy-Meir, I. (1975). Stability of grazing systems: an application of predator–prey graphs. *Journal of Ecology* **63**, 459–483.

Rinaldi, S. and Muratori, S. (1992*a*). Limit cycles in slow–fast forest-pest models. *Theoretical Population Biology* **41**, 26–43.

Rinaldi, S. and Muratori, S. (1992*b*). Slow–fast limit cycles in predator–prey models. *Ecological Modelling* **61**, 287–308.

Rinaldi, S., Soncini-Sessa, R., Stehfest, H. and Tamura, H. (1979). *Modeling and Control of River Quality.* London: McGraw-Hill.

Strogatz, S. H. (1994). *Nonlinear Dynamics and Chaos.* Reading, MA: Addison-Wesley.

United Nations Economic Commission for Europe. (1994). Protocol to the 1979 convention on long-range transboundary air pollution on further reduction of sulphur emissions. Geneva, Switzerland.

Walters, C. (1986). *Adaptive Management of Renewable Resources.* New York: Macmillan.

Appendix

This Appendix shows that model (1, 2) with constant C cannot have strictly positive limit cycles. The proof is a simple application of *Dulac*'s criterion for non-existence of limit cycles. Such a criterion says the following (Strogatz, 1994): "Let $\dot{x} = \boldsymbol{F}(\boldsymbol{x})$ be a continuously differentiable vector field defined on a simply connected subset S of the plane. If there exists a continuousy differentiable, real-valued function $g(\boldsymbol{x})$ such that the divergence of $g(\boldsymbol{x})\boldsymbol{F}(\boldsymbol{x})$ has one sign throughout S, then there are no closed orbits lying entirely in S."

In our case the function g exists since:

$$g(R, P) = \frac{1}{R}$$

gives,

$$g\boldsymbol{F} = \left| \begin{array}{c} (1-R) - M(P) + \dfrac{s}{R} \\[2mm] \dfrac{wD(C)}{R} - \dfrac{aP}{R} - bP \end{array} \right|$$

so that,

$$div[g\boldsymbol{F}] = -1 - \frac{s}{R^2} - \frac{a}{R} - b$$

which is strictly negative inside the positive quadrant. Therefore, no strictly positive limit cycle exists.